
On the coupling of finite volume and discontinuous Galerkin method for elliptic problems

Prince Chidyagwai · Ilya Mishev · Béatrice Rivière

March 15, 2010

Abstract The coupling of cell-centered finite volume method with primal discontinuous Galerkin method is introduced in this paper for elliptic problems. Convergence of the method with respect to the mesh size is proved. Numerical examples confirm the theoretical rates of convergence. Advantages of the coupled scheme are shown for problems with discontinuous coefficients or anisotropic diffusion matrix.

Keywords discontinuous Galerkin · finite volume · anisotropic medium · multi-
numerics · convergence

1 Introduction

This paper presents a multinumerics scheme for solving the elliptic problem, that combines the primal Discontinuous Galerkin (DG) and cell-centered Finite Volume (FV) methods. Applications of this work are of interest for modeling fluid flow in porous media. Our proposed scheme takes advantage of both the accuracy of DG in regions of interest, such as regions containing local features (shales, pinch-outs) and the efficiency of FV in the rest of the domain.

Over the last ten years, primal discontinuous Galerkin methods have been shown to be accurate for flow problems in heterogeneous porous media [24,23]. The fact that that DG methods are locally conservative makes them an attractive scheme for simulating more complicated flow and transport problems, such as multiphase flows [2,21,5,15,17]. The flexibility of DG methods allows for general unstructured meshes and discontinuous coefficients. In addition, accuracy can be increased by an easy use of local mesh refinement and high order polynomials.

P. Chidyagwai

Rice University, Department of Computational and Applied Mathematics, 6100 Main St MS-134, Houston, TX 77005, U.S.A. E-mail: prince.chidyagwai@rice.edu

I. Mishev

ExxonMobil Upstream Research Company, 3120 Buffalo Speedway, Houston, TX 77098, U.S.A. E-mail: ilya.d.mishev@exxonmobil.com

B. Rivière

Rice University, Department of Computational and Applied Mathematics, 6100 Main St MS-134, Houston, TX 77005, U.S.A. E-mail: riviere@caam.rice.edu

Another locally conservative method is the class of finite volume methods. In addition to the local mass conservation property, FV methods are robust schemes that can be used on very general geometries with structured or unstructured meshes. Vertex-centered FV methods on unstructured meshes are analyzed in [1,4,3]. Cell-centered FV methods on triangular or Voronoi meshes are studied for instance in [9,8,14,25,10]. Applications of FV methods to multiphase flow in porous media are addressed in [7,13,11,12]. These methods produce monotone discretizations, handle well the discontinuous coefficients, and are computationally very efficient. Unfortunately, the convergence of the cell-centered FV methods is guaranteed only on specially constructed grids (Voronoi meshes) and for problems with no mixed second derivatives. Local refinement is very difficult on Voronoi grids and usually cannot be done dynamically because of the global nature of the Voronoi grids. Modeling real flows in porous media with complicated geological features like faults, disappearing layers (pinch-outs), etc., and multiple complex wells essentially transfer the difficulty to the grid generation. Coupling of FV and DG discretizations can considerably alleviate the requirement for the grid with an acceptable increase of the computational cost. Moreover, the accuracy of the computed solution also could be improved. We show in Example 2 how DG can be used around the pinch-outs where constructing a Voronoi grid aligned with the layers is very difficult. Another application is in the areas where the principal directions of the permeability is not aligned with the grid as shown in Example 3. Using only FV in such application will produce a wrong solution. Both examples demonstrate the use of DG for local refinement. Cell-centered FV methods are currently widely used in most of the production reservoir simulators. Coupling of FV and DG methods produces a more flexible discretization with improved approximation properties.

An outline of the paper is now given. In the following section, the numerical method is formulated for a general elliptic problem. Then, a priori error estimates are derived in Section 3. Numerical examples are shown in Section 4. Conclusions follow.

2 Model Problem And Scheme

Let $\Omega \in \mathbb{R}^d$, $d = 2, 3$, be a bounded polygonal domain subdivided into non overlapping subdomains Ω_F^i and Ω_D^i and let $\Omega_F = \cup_i \Omega_F^i$ and $\Omega_D = \cup_i \Omega_D^i$. The numerical method discussed in this paper uses a finite volume method on Ω_F and a discontinuous Galerkin method on Ω_D . Let $f \in L^2(\Omega)$ and $g \in H^{1/2}(\partial\Omega)$. The solution u of the elliptic problem satisfies

$$-\nabla \cdot (K \nabla u) = f, \quad \text{in } \Omega, \quad (1)$$

$$u = g, \quad \text{on } \partial\Omega. \quad (2)$$

The coefficient K is bounded above and below by positive constants k_1 and k_0 respectively. Let \mathcal{E}_D^h (resp. \mathcal{E}_F^h) be a subdivision of Ω_D (resp. Ω_F), made of cells V (Voronoi cells in Ω_F and either triangles/tetrahedra/hexahedra or Voronoi cells in Ω_D). We also denote by h_F (resp. h_D) the maximum diameter over all cells in Ω_F (resp. Ω_D) and we let $h = \max(h_F, h_D)$. We assume that the meshes match at the interface $\Gamma_{DF} = \partial\Omega_D \cap \partial\Omega_F$.

The definition of the mesh \mathcal{E}_F^h requires further notation. We assume that \mathcal{E}_F^h is an admissible finite volume mesh, in the following sense:

1. There is a family of nodes $\{x_V\}_{V \in \mathcal{E}_F^h}$ such that $x_V \in \bar{V}$ and if an edge γ is such that $\gamma = \partial V \cap \partial W$ with $W \neq V$, it is assumed that $x_W \neq x_V$ and that the straight line going through x_V and x_W is orthogonal to γ .
2. For any boundary edge $\gamma = \partial V \cap \partial \Omega$ with $V \in \mathcal{E}_F^h$, it is assumed that $x_V \notin \gamma$. However this condition can be relaxed (see Remark 1 in Section 3). Let y_γ be the (non-empty) intersection between the straight line going through x_V and orthogonal to γ .

We denote by $\Gamma_F^{h,\mathcal{I}}$ the set of edges that belong to the interior of Ω_F and by $\Gamma_F^{h,\partial}$ the set of boundary edges that belong to $\partial\Omega_F \cap \partial\Omega$. Similarly, the sets of edges that belong to the interior of Ω_D and boundary edges that belong to $\partial\Omega_D \cap \partial\Omega$ are denoted by $\Gamma_D^{h,\mathcal{I}}$ and $\Gamma_D^{h,\partial}$ respectively. We also define

$$\Gamma_F^h = \Gamma_F^{h,\mathcal{I}} \cup \Gamma_F^{h,\partial}, \quad \Gamma_D^h = \Gamma_D^{h,\mathcal{I}} \cup \Gamma_D^{h,\partial}.$$

There remains the set of edges that belong to the interface Γ_{DF} ; this particular set is denoted by Γ_{DF}^h .

We now define a parameter d_γ that is associated to each edge in the FV mesh. Let V and W be two cells in the FV region such that $\gamma = \partial V \cap \partial W$ is an interior edge. We define the parameter d_γ to be the Euclidean distance between the nodes x_V and x_W .

$$d_\gamma = d(x_V, x_W).$$

If the edge γ is a boundary edge (i.e. belongs to $\partial V \cap \partial \Omega$) the parameter d_γ is the distance between the node x_V and the edge γ .

$$d_\gamma = d(x_V, \gamma) = d(x_V, y_\gamma).$$

Next, assume that an edge γ is the intersection of a FV cell V and a DG cell W . The parameter d_γ is defined to be the distance between the node x_V and the point y_γ , which is (as in the boundary case) the intersection between the straight line going through x_V and orthogonal to γ . Here, we have made the assumption that x_V does not lie on the interface γ . Assume there is some $\theta > 0$ such that

$$\forall \gamma \in \Gamma_F^{h,\mathcal{I}}, \quad \gamma = \partial V \cap \partial W, \quad d_\gamma \geq \theta \max(h_V, h_W),$$

$$\forall \gamma \in \Gamma_F^{h,\partial}, \quad \gamma = \partial V \cap \partial \Omega, \quad d_\gamma \geq \theta h_V,$$

$$\forall \gamma \in \Gamma_{DF}^h, \quad \gamma = \partial V \cap \partial W, \quad V \in \mathcal{E}_F^h, \quad W \in \mathcal{E}_D^h, \quad d_\gamma \geq \theta h_V.$$

Finally, we define the harmonic average of the diffusion coefficient:

$$\forall \gamma \in \Gamma_F^{h,\mathcal{I}}, \quad \gamma = \partial V \cap \partial W, \quad K_\gamma = d_\gamma \left| \int_{x_V}^{x_W} \frac{ds}{K(s)} \right|^{-1},$$

$$\forall \gamma \in \Gamma_F^{h,\partial}, \quad \gamma = \partial V \cap \partial \Omega, \quad K_\gamma = d_\gamma \left| \int_{x_V}^{y_\gamma} \frac{ds}{K(s)} \right|^{-1},$$

$$\forall \gamma \in \Gamma_{DF}^h, \quad \gamma = \partial V \cap \partial W, \quad V \in \mathcal{E}_F^h, \quad W \in \mathcal{E}_D^h, \quad K_\gamma = d_\gamma \left| \int_{x_V}^{y_\gamma} \frac{ds}{K(s)} \right|^{-1}.$$

It is easy to see that K_γ is also bounded above and below by k_1 and k_0 respectively.

We denote by $|\gamma|$ the length of an edge γ . The finite dimensional space consists of piecewise polynomials of degree less than or equal to r in the DG region and of degree equal to zero in the FV region.

$$X^h = \{v \in L^2(\Omega) : v|_V \in \mathbb{P}_r(V) \quad \forall V \in \mathcal{E}_D^h, \quad v|_V \in \mathbb{P}_0(V) \quad \forall V \in \mathcal{E}_F^h\}.$$

Define the jump of a function in X^h . For any edge γ we fix a unit normal vector \mathbf{n}_γ to γ . We assume that if γ is a boundary edge (belongs to $\partial\Omega$), then \mathbf{n}_γ points outward of $\partial\Omega$. If γ belongs to the interface Γ_{DF}^h , then we assume that \mathbf{n}_γ points from the DG region into the FV region. Let us denote by V and W the mesh elements so that the vector \mathbf{n}_γ points from ∂V into ∂W . We define the jump of a function $u \in X^h$.

$$\begin{aligned} \gamma \in \Gamma_F^{h,\mathcal{I}}, \quad [u]|_\gamma &= u(x_V) - u(x_W), \\ \gamma \in \Gamma_D^{h,\mathcal{I}}, \quad [u]|_\gamma &= u|_V - u|_W, \\ \gamma \in \Gamma_{DF}^h, \quad [u]|_\gamma &= u|_{\Omega_D}(y_\gamma) - u|_{\Omega_F}(x_W), \\ \gamma \in \Gamma_F^{h,\partial}, \quad [u]|_\gamma &= u(x_V), \\ \gamma \in \Gamma_D^{h,\partial}, \quad [u]|_\gamma &= u|_V. \end{aligned}$$

We remark that the quantity $[u]|_\gamma$ is a number except for the edges $\gamma \in \Gamma_D^h$. The DG method requires additional notation. Let $\{u\}$ denote the average of a function $u \in X^h$.

$$\begin{aligned} \gamma \in \Gamma_D^{h,\mathcal{I}}, \quad \gamma = \partial V \cap \partial W, \quad u|_\gamma &= 0.5(u|_V + u|_W), \\ \gamma \in \Gamma_D^{h,\partial}, \quad \gamma \in \partial V, \quad \{u\}|_\gamma &= u. \end{aligned}$$

Let $\sigma > 0$ denote the penalty parameter and $\epsilon \in \{-1, 1\}$ be the symmetrization parameter. For a given edge γ shared by two mesh elements V and W , let $h_\gamma = \max(\text{diam}(V), \text{diam}(W))$. The DG bilinear form is for all $u, v \in X^h$

$$\begin{aligned} a_D(u, v) &= \sum_{V \in \mathcal{E}_D^h} \int_V K \nabla u \cdot \nabla v - \sum_{\gamma \in \Gamma_D^h} \int_\gamma \{K \nabla u \cdot \mathbf{n}_\gamma\} [v] \\ &+ \epsilon \sum_{\gamma \in \Gamma_D^h} \int_\gamma \{K \nabla v \cdot \mathbf{n}_\gamma\} [u] + \sum_{\gamma \in \Gamma_D^h} \frac{\sigma}{h_\gamma} \int_\gamma [u][v]. \end{aligned} \quad (3)$$

The cell-centered finite volume method is defined by the following bilinear form for all $u, v \in X^h$

$$a_F(u, v) = \sum_{\gamma \in \Gamma_F^h} \frac{|\gamma|}{d_\gamma} K_\gamma [u][v]. \quad (4)$$

Our scheme uses the overall bilinear form for all $u, v \in X^h$

$$a(u, v) = a_D(u, v) + a_F(u, v) + a_{DF}(u, v), \quad (5)$$

where a_{DF} is the coupling form at the interface Γ_{FD}^h :

$$a_{DF}(u, v) = \sum_{\gamma \in \Gamma_{FD}^h} \frac{|\gamma|}{d_\gamma} K_\gamma [u][v]. \quad (6)$$

The source functions and boundary conditions are taken into account in the form

$$\forall v \in X^h, \quad \ell(v) = \int_{\Omega} f v + \epsilon \sum_{\gamma \in \Gamma_D^{h,\partial}} \int_{\gamma} (K \nabla v \cdot \mathbf{n}_{\gamma} + \frac{\sigma}{h_{\gamma}} v) g + \sum_{\gamma \in \Gamma_F^{h,\partial}} K_{\gamma} \frac{|\gamma|}{d_{\gamma}} g(y_{\gamma}) v. \quad (7)$$

The numerical scheme is: to find $U \in X^h$ satisfying

$$\forall v \in X^h, \quad a(U, v) = \ell(v) \quad (8)$$

We next define some norms, that naturally arise from the bilinear forms above:

$$\|v\|_{DG} = \left(\sum_{V \in \mathcal{E}_D^h} \|K^{1/2} \nabla v\|_{L^2(V)}^2 + \sum_{\gamma \in \Gamma_D^h} h_{\gamma}^{-1/2} \|[v]\|_{L^2(\gamma)}^2 \right)^{1/2}, \quad (9)$$

$$\|v\|_{FV} = \left(\sum_{\gamma \in \Gamma_F^h} \frac{|\gamma|}{d_{\gamma}} K_{\gamma} [v]^2 \right)^{1/2}, \quad (10)$$

$$\|v\|_{\mathcal{E}} = \left(\|v\|_{DG}^2 + \|v\|_{FV}^2 + \sum_{\gamma \in \Gamma_{FD}^h} \frac{K_{\gamma}}{d_{\gamma}} [v]^2 \right)^{1/2}. \quad (11)$$

We now give some important properties of the bilinear forms.

Lemma 1 *There exist α, β positive constants independent of h such that*

$$\forall v \in X^h, \quad a_D(v, v) \geq \alpha \|v\|_{DG}^2, \quad (12)$$

$$\forall v \in X^h, \quad a_F(v, v) = \|v\|_{FV}^2, \quad (13)$$

$$\forall v \in X^h, \quad a(v, v) \geq \beta \|v\|_{\mathcal{E}}^2. \quad (14)$$

Proof Inequality (12) is well known and requires the penalty parameter σ to be large enough if $\epsilon = -1$ [22]. Inequality (13) is trivial and the third inequality is a straightforward consequence of the first two and the definition (5).

Lemma 2 *There exists a unique solution $U \in X^h$ satisfying (8).*

Proof It suffices to show uniqueness of U satisfying (8) with $f = g = 0$. Take $v = U$ in (8), and use coercivity of a . This implies that $\|U\|_{\mathcal{E}} = 0$ and thus $U = 0$ in X^h .

3 Error Analysis

For simplicity proofs are given in the case where there are only one DG region and one FV region, but the proofs for the general case are similar. For each edge γ we define a subdomain \mathcal{V}_{γ} as follows. Assume that $\gamma \in \Gamma_{FD}^{h,\mathcal{I}}$ with $\gamma = \partial V \cap \partial W$. Define

$$\mathcal{V}_{W,\gamma} = \{tx_V + (1-t)x, \quad x \in \gamma, \quad t \in [0, 1]\},$$

and let

$$\mathcal{V}_{\gamma} = \mathcal{V}_{W,\gamma} \cap \mathcal{V}_{V,\gamma}.$$

Assume now that $\gamma \in \Gamma_F^{h,\partial}$ with $\gamma \subset \partial W$, then $\mathcal{V}_{\gamma} = \mathcal{V}_{W,\gamma}$. Finally if $\gamma \in \Gamma_{DF}^h$ with $\gamma = \partial V \cap \partial W$, and $W \in \mathcal{E}_F^h$, then $\mathcal{V}_{\gamma} = \mathcal{V}_{W,\gamma}$.

Lemma 3 Define the residuals for any $u \in H^2(\Omega)$.

$$\gamma \in \Gamma_F^{h,\mathcal{I}} \quad R_\gamma(u) = -\frac{|\gamma|}{d_\gamma} K_\gamma[u] - \int_\gamma K \nabla u \cdot n_\gamma, \quad (15)$$

$$\gamma \in \Gamma_F^{h,\partial}, \quad \gamma = \partial V \cap \partial \Omega \quad R_\gamma(u) = -\frac{|\gamma|}{d_\gamma} K_\gamma(u(x_V) - g(y_\gamma)) - \int_\gamma K \nabla u \cdot n_\gamma, \quad (16)$$

$$\forall \gamma \in \Gamma_{DF}^h, \quad R_\gamma(u) = -K \nabla u \cdot n_\gamma - \frac{K_\gamma}{d_\gamma}[u]. \quad (17)$$

Let $H(u)$ denote the Hessian matrix of u . Assume K is a positive constant. Then, there exists a constant C independent of h and u , but dependent on θ , such that

$$\gamma \in \Gamma_F^h, \quad |R_\gamma(u)|^2 \leq C \frac{h_F^2 |\gamma|}{d_\gamma} \int_{\mathcal{V}_\gamma} |H(u)|^2, \quad (18)$$

$$\gamma \in \Gamma_{DF}^h, \quad \left(\int_\gamma |R_\gamma(u)| \right)^2 \leq C \frac{h_F^2 |\gamma|}{d_\gamma} \int_{\mathcal{V}_\gamma} |H(u)|^2. \quad (19)$$

Proof Inequalities (18) and (19) can be found in [6].

The following result shows that there is a consistency error only due to the FV discretization. In the DG region, there is no consistency error.

Lemma 4 Let $u \in H^1(\Omega) \cap H^2(\mathcal{E}^h)$ be the solution to problem (1)-(2). Then u satisfies

$$\begin{aligned} \forall v \in X^h, \quad a(u, v) = \ell(v) - \sum_{\gamma \in \Gamma_F^h} R_\gamma(u)[v] - \sum_{\gamma \in \Gamma_{DF}^h} [v] \int_\gamma R_\gamma(u) \\ - \sum_{\gamma \in \Gamma_{DF}^h} \int_\gamma R_\gamma(u)(v|_{\Omega_D} - v|_{\Omega_D}(y_\gamma)) + \sum_{\gamma \in \Gamma_{DF}^h} \frac{|\gamma| K_\gamma}{d_\gamma}[u] \left(v|_{\Omega_D}(y_\gamma) - |\gamma|^{-1} \int_\gamma v|_{\Omega_D} \right). \end{aligned} \quad (20)$$

Proof Let $V \in \mathcal{E}_F^h$ and let $v \in X^h$ such that $v|_V = 1$ and $v = 0$ elsewhere. Denote by n_V the outward unit normal to V . Multiply (1) by v and integrate on V by parts:

$$- \int_{\partial V} K \nabla u \cdot n_V v = \int_V f v,$$

or

$$- \sum_{\gamma \in \partial V} \int_\gamma K \nabla u \cdot n_V v = \int_V f v. \quad (21)$$

Summing (21) over all FV cells, and using the residual definitions, we obtain for all $v \in X^h$:

$$a_F(u, v) + \sum_{\gamma \in \Gamma_{DF}^h} \int_\gamma K \nabla u \cdot n_\gamma v_{FV} + \sum_{\gamma \in \Gamma_F^h} R_\gamma(u)[v] - \sum_{\gamma \in \Gamma_F^{h,\partial}} \frac{|\gamma|}{d_\gamma} K_\gamma g(y_\gamma) v = \int_{\Omega_F} f v. \quad (22)$$

For readability, we denote by v_{DG} the restriction of v to the DG region and by v_{FV} its restriction to the FV region. Next, we consider $V \in \mathcal{E}_D^h$, multiply (1) by $v \in X^h$ and integrate by parts:

$$\int_V K \nabla u \cdot \nabla v - \int_{\partial V} K \nabla u \cdot n_V v = \int_V f v.$$

Sum over all V in the DG region, add the stabilization terms to obtain

$$a_D(u, v) - \sum_{\gamma \in \Gamma_{DF}^h} \int_{\gamma} K \nabla u \cdot \mathbf{n}_{\gamma} v_{DG} = \int_{\Omega_D} f v + \epsilon \sum_{\gamma \in \Gamma_D^{h,\partial}} \int_{\gamma} (K \nabla v \cdot \mathbf{n}_{\gamma} + \frac{\sigma}{h_{\gamma}} v) g. \quad (23)$$

We now add (22) and (23):

$$a_F(u, v) + a_D(u, v) + T = \ell(v) - \sum_{\gamma \in \Gamma_F^h} R_{\gamma}(u)[v],$$

where T corresponds to the terms involving integrals on the interface Γ_{DF} . We can write using the regularity of the solution u (namely the fact that $u \in H^2(\Omega)$):

$$T = - \sum_{\gamma \in \Gamma_{DF}^h} \int_{\gamma} K \nabla u \cdot \mathbf{n}_{\gamma} (v_{DG} - v_{FV}) = - \sum_{\gamma \in \Gamma_{DF}^h} \int_{\gamma} K \nabla u \cdot \mathbf{n}_{\gamma} (v_{DG} - v_{DG}(y_{\gamma})) - \sum_{\gamma \in \Gamma_{DF}^h} [v] \int_{\gamma} K \nabla u \cdot \mathbf{n}_{\gamma}.$$

Using the definition of the residual in Lemma 3, we obtain

$$T = \sum_{\gamma \in \Gamma_{DF}^h} \int_{\gamma} (R_{\gamma}(u) + \frac{K_{\gamma}}{d_{\gamma}} [u]) (v_{DG} - v_{DG}(y_{\gamma})) + \sum_{\gamma \in \Gamma_{DF}^h} [v] \int_{\gamma} (R_{\gamma}(u) + \frac{K_{\gamma}}{d_{\gamma}} [u]),$$

or

$$T = a_{DF}(u, v) + \sum_{\gamma \in \Gamma_{DF}^h} [v] \int_{\gamma} R_{\gamma}(u) + \sum_{\gamma \in \Gamma_{DF}^h} \int_{\gamma} R_{\gamma}(u) (v_{DG} - v_{DG}(y_{\gamma})) - \sum_{\gamma \in \Gamma_{DF}^h} \frac{|\gamma| K_{\gamma}}{d_{\gamma}} [u] E(v_{DG}),$$

with

$$E(v_{DG}) = v_{DG}(y_{\gamma}) - \frac{1}{|\gamma|} \int_{\gamma} v_{DG}.$$

Thus we can conclude.

Theorem 1 *Assume that $u \in H^2(\Omega)$ and that $u|_{\Omega_D} \in H^{r+1}(\mathcal{E}_D^h)$ for $r \geq 1$. Under the assumptions of Lemma 3, there exists a constant C independent of h_D and h_F such that*

$$\|U - u\|_{\mathcal{E}} \leq C(h_D^r + h_F).$$

Proof We can write

$$U - u = \chi - \xi, \quad \chi = U - \tilde{u}, \quad \xi = u - \tilde{u}.$$

The function $\tilde{u} \in X^h$ is chosen so that

$$\forall V \in \mathcal{E}_F^h, \quad \tilde{u}|_V = u(x_V). \quad (24)$$

On the DG region \tilde{u} is assumed to satisfy the usual approximation properties. Using the definition of the scheme (8) and Lemma 4, we obtain an error equation:

$$\begin{aligned} a(\chi, \chi) &= a(\xi, \chi) + \sum_{\gamma \in \Gamma_F^h} R_{\gamma}(u)[\chi] + \sum_{\gamma \in \Gamma_{DF}^h} [\chi] \int_{\gamma} R_{\gamma}(u) + \sum_{\gamma \in \Gamma_{DF}^h} \int_{\gamma} R_{\gamma}(u) (\chi|_{\Omega_D} - \chi|_{\Omega_D}(y_{\gamma})) \\ &\quad + \sum_{\gamma \in \Gamma_{DF}^h} \frac{|\gamma| K_{\gamma}}{d_{\gamma}} [u] \left(\chi|_{\Omega_D}(y_{\gamma}) - |\gamma|^{-1} \int_{\gamma} \chi|_{\Omega_D} \right). \end{aligned}$$

Let us estimate the terms in the right hand side. Since $\xi(x_V) = 0$ for all nodes x_V in Ω_F , we have

$$a(\xi, \chi) = a_D(\xi, \chi) + a_F(\xi, \chi) + a_{DF}(\xi, \chi) = a_D(\xi, \chi) + a_{DF}(\xi, \chi).$$

We can use standard techniques to bound $a_D(\xi, \chi)$. The other term reduces to

$$a_{DF}(\xi, \chi) = \sum_{\gamma \in \Gamma_{DF}^h} \frac{|\gamma|K_\gamma}{d_\gamma} [\chi] \xi|_{\Omega_D}(y_\gamma).$$

We claim that we can choose the approximation \tilde{u} such that $\xi|_{\Omega_D}(y_\gamma) = 0$. In that case we have $a_{DF}(\xi, \chi) = 0$. The first consistency error term is bounded as follows:

$$\sum_{\gamma \in \Gamma_F^h} R_\gamma(u)[\chi] \leq \frac{1}{16} \sum_{\gamma \in \Gamma_F^h} \frac{|\gamma|K_\gamma}{d_\gamma} [\chi]^2 + 4 \sum_{\gamma \in \Gamma_F^h} \frac{d_\gamma}{|\gamma|} (R_\gamma(u))^2.$$

Using the bound (18) and denoting by $H(u)$ the Hessian matrix of u , we have

$$\sum_{\gamma \in \Gamma_F^h} R_\gamma(u)[\chi] \leq \frac{1}{16} \sum_{\gamma \in \Gamma_F^h} \frac{|\gamma|K_\gamma}{d_\gamma} [\chi]^2 + Ch_F^2 \int_{\Omega_F} |H(u)|^2.$$

The second consistency error term is as:

$$\sum_{\gamma \in \Gamma_{DF}^h} [\chi] \int_\gamma R_\gamma(u) \leq \frac{1}{16} \sum_{\gamma \in \Gamma_{DF}^h} \frac{|\gamma|K_\gamma}{d_\gamma} [\chi]^2 + 4 \sum_{\gamma \in \Gamma_{DF}^h} \frac{d_\gamma}{|\gamma|} \left(\int_\gamma R_\gamma(u) \right)^2.$$

which with the bound (19) gives:

$$\sum_{\gamma \in \Gamma_{DF}^h} [\chi] \int_\gamma R_\gamma(u) \leq \frac{1}{16} \sum_{\gamma \in \Gamma_{DF}^h} \frac{|\gamma|K_\gamma}{d_\gamma} [\chi]^2 + Ch_F^2 \int_{\Omega_F} |H(u)|^2.$$

Finally we have

$$\sum_{\gamma \in \Gamma_{DF}^h} \int_\gamma R_\gamma(u) (\chi|_{\Omega_D} - \chi|_{\Omega_D}(y_\gamma)) \leq \sum_{\gamma \in \Gamma_{DF}^h} \int_\gamma |R_\gamma(u)| |\chi|_{\Omega_D} - \chi|_{\Omega_D}(y_\gamma)|.$$

Let us fix an edge $\gamma \in \Gamma_{DG}^h$ with $\gamma = \partial V \cap \partial W$, and $V \in \mathcal{E}_D^h$. Let us denote by $\eta = \chi|_V - \chi|_V(y_\gamma)$. Then we have by trace and inverse inequalities:

$$\|\eta\|_{L^\infty(\gamma)} \leq Ch_D^{-1/2} \|\eta\|_{L^2(\gamma)} \leq C \|\nabla \eta\|_{L^2(V)}.$$

Therefore we obtain

$$\begin{aligned} \sum_{\gamma \in \Gamma_{DF}^h} \int_\gamma R_\gamma(u) (\chi|_{\Omega_D} - \chi|_{\Omega_D}(y_\gamma)) &\leq \frac{1}{16} \|\chi\|_{DG}^2 + C \sum_{\gamma \in \Gamma_{DF}^h} \left(\int_\gamma |R_\gamma(u)| \right)^2 \\ &\leq \frac{1}{16} \|\chi\|_{DG}^2 + Ch_F^2 \int_{\Omega_F} |H(u)|^2. \end{aligned}$$

The last consistency error term is bounded as follows. Fix an edge in Γ_{DF}^h such that $\gamma = \partial V \cap \partial W$ with $V \in \mathcal{E}_D^h$:

$$\frac{|\gamma|K_\gamma}{d_\gamma}[u] \left(\chi|_{\Omega_D}(y_\gamma) - |\gamma|^{-1} \int_\gamma \chi|_{\Omega_D} \right) \leq C \|\nabla \chi\|_{L^2(V)} \frac{|\gamma|K_\gamma}{d_\gamma} |[u]|.$$

Using the density of C^1 into H^2 and a Taylor expansion, we can prove that:

$$|[u]|_\gamma \leq d_\gamma |\gamma|^{1/2} \|\nabla u \cdot \mathbf{n}\|_{L^2(\gamma)}.$$

So we have

$$\begin{aligned} \sum_{\gamma \in \Gamma_{DF}^h} \frac{|\gamma|K_\gamma}{d_\gamma}[u] \left(\chi|_{\Omega_D}(y_\gamma) - |\gamma|^{-1} \int_\gamma \chi|_{\Omega_D} \right) &\leq \frac{1}{16} \|\chi\|_{DG}^2 + Ch_F^3 \|\nabla u \cdot \mathbf{n}\|_{L^2(\Gamma_{DF}^h)}^2 \\ &\leq \frac{1}{16} \|\chi\|_{DG}^2 + Ch_F^2 \|u\|_{H^2(\Omega_F)}^2. \end{aligned}$$

We can then conclude.

Remark 1: The results of Theorem 1 are still valid if there are some nodes x_V located on boundary edges $\gamma \in \Gamma_F^{h,\partial}$. Let denote by $\Gamma_F^{h,0}$ the set of such edges. The coupled scheme is slightly modified. The discrete space is the set Y^h of functions $v \in X^h$ such that $v(x_V) = 0$ for all $x_V \in \Gamma_F^{h,0}$. The bilinear form a_F and linear form ℓ become

$$\begin{aligned} a_F(u, v) &= \sum_{\gamma \in \Gamma_F^h \setminus \Gamma_F^{h,0}} \frac{|\gamma|}{d_\gamma} K_\gamma [u][v] \\ \ell(v) &= \int_\Omega f v + \epsilon \sum_{\gamma \in \Gamma_D^{h,\partial}} \int_\gamma (K \nabla v \cdot \mathbf{n}_\gamma + \frac{\sigma}{h_\gamma} v) g + \sum_{\gamma \in \Gamma_F^{h,\partial} \setminus \Gamma_F^{h,0}} K_\gamma \frac{|\gamma|}{d_\gamma} g(y_\gamma) v. \end{aligned}$$

The solution $U \in X^h$ is such that $U(x_V) = g(x_V)$ for all $x_V \in \Gamma_F^{h,0}$, and satisfies

$$\forall v \in Y^h, \quad a(U, v) = \ell(v)$$

4 Numerical Examples

In the following section we present examples that verify the convergence rates for the proposed FV-DG coupling and illustrate cases in which the coupled scheme yields a more accurate solution.

Example 1 Convergence Study

First we consider the unit square domain Ω partitioned into two subdomains Ω_D and Ω_F (see Fig. 1). The boundary conditions are chosen so that the exact solution $u(x, y) = (x^2 - x)(y^2 - y)$ and the coefficient K is equal to one.

In order to perform the convergence tests we generate five Delaunay triangulations using the software EasyMesh developed by Bojan Niceno [16]. At each level of refinement we ensure that the maximum area of each triangle decreases by a factor of 4. We then generate the dual Voronoi mesh for each Delaunay triangulation. This technique has been used in [14]. Fig. 1 shows an example of the mesh for the convergence test with 340 Voronoi cells. The shaded subdomain is Ω_D on which the solution is approximated

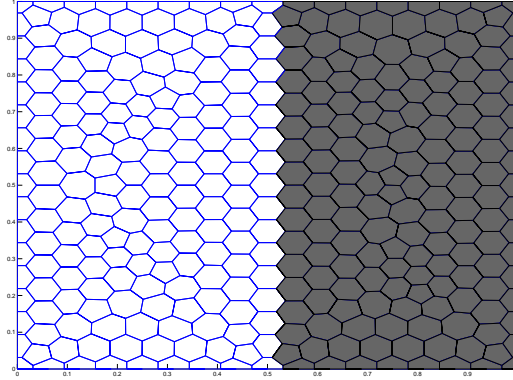


Fig. 1: Computational mesh with 340 Voronoi cells: Ω_F is the white region and Ω_D is the grey region.

using the discontinuous Galerkin method and the rest of the domain is Ω_{FV} , on which the finite volume method is used. The DG parameters are chosen as: $\sigma = 1, \epsilon = 1$.

Fig. 2 shows the exact solution and the numerical solution obtained on the mesh shown in Fig. 1. We observe the expected clear distinction between the piecewise constant solution on Ω_F and the smoother solution on Ω_D on which the solution is approximated by discontinuous quadratic polynomials.

| N | $\ U - u\ _{0,FV}$ | $\ U - u\ _{FV}$ | $\ U - u\ _{L^2(\Omega_D)}$ | $\ U - u\ _{DG}$ | $\ U - u\ _{\mathcal{E}}$ |
|------|------------------------|------------------------|-----------------------------|------------------------|---------------------------|
| 31 | 1.489×10^{-3} | 1.034×10^{-2} | 1.147×10^{-3} | 3.049×10^{-2} | 3.872×10^{-3} |
| 102 | 4.010×10^{-4} | 2.748×10^{-3} | 3.034×10^{-4} | 1.503×10^{-2} | 1.781×10^{-3} |
| 340 | 1.033×10^{-4} | 8.143×10^{-4} | 8.386×10^{-5} | 8.031×10^{-3} | 9.276×10^{-4} |
| 1272 | 2.609×10^{-5} | 2.722×10^{-4} | 2.112×10^{-5} | 4.039×10^{-3} | 4.653×10^{-4} |
| 4895 | 6.496×10^{-6} | 1.016×10^{-4} | 5.322×10^{-6} | 2.039×10^{-3} | 2.313×10^{-4} |
| rate | 2.00 | 1.40 | 2.00 | 1.00 | 1.00 |

Table 1: Numerical errors and convergence rates for DG scheme of order one coupled with FV.

| N | $\ U - u\ _{0,FV}$ | $\ U - u\ _{FV}$ | $\ U - u\ _{L^2(\Omega_D)}$ | $\ U - u\ _{DG}$ | $\ U - u\ _{\mathcal{E}}$ |
|------|------------------------|------------------------|-----------------------------|------------------------|---------------------------|
| 31 | 9.479×10^{-4} | 6.592×10^{-3} | 4.881×10^{-4} | 4.298×10^{-3} | 2.172×10^{-3} |
| 102 | 2.593×10^{-4} | 1.872×10^{-3} | 1.176×10^{-4} | 1.598×10^{-3} | 9.009×10^{-4} |
| 340 | 6.578×10^{-5} | 6.148×10^{-4} | 4.028×10^{-5} | 7.550×10^{-4} | 4.415×10^{-4} |
| 1272 | 1.744×10^{-5} | 2.389×10^{-4} | 9.198×10^{-6} | 4.328×10^{-4} | 2.397×10^{-4} |
| 4895 | 4.766×10^{-6} | 1.012×10^{-4} | 2.487×10^{-6} | 1.120×10^{-4} | 1.198×10^{-4} |
| rate | 1.88 | 1.23 | 1.89 | 1.95 | 1.00 |

Table 2: Numerical errors and convergence rates for DG scheme of order two coupled with FV.

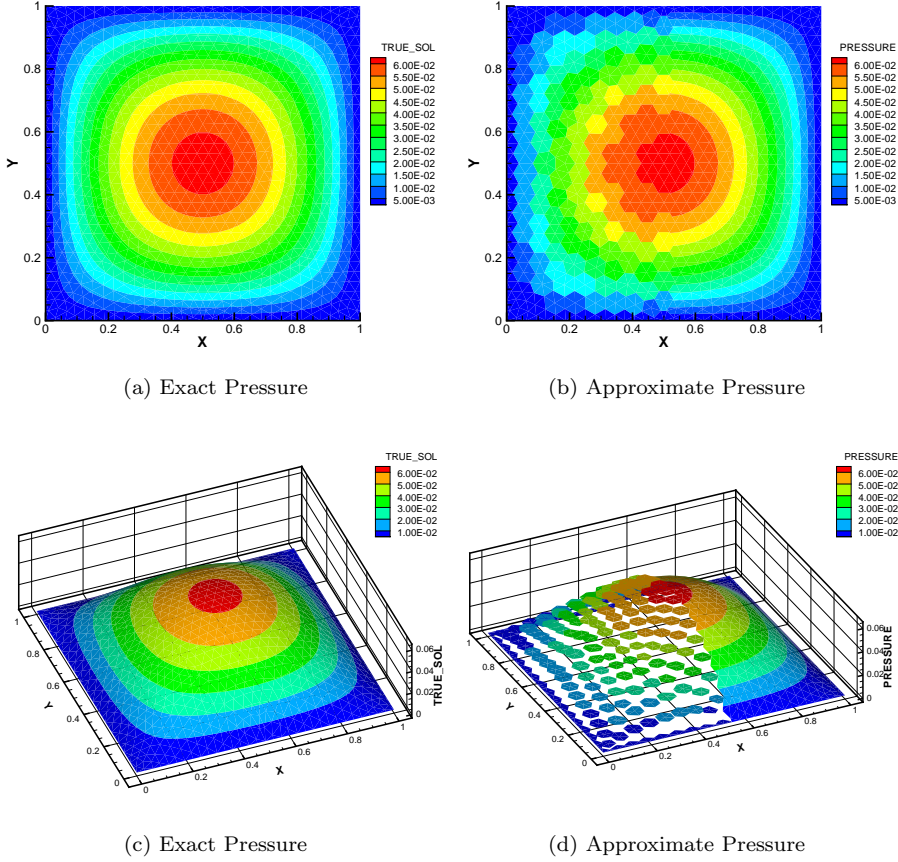


Fig. 2: Contours of exact and numerical solutions for example 1.

Tables 1 and 2 show the expected convergence rate of $O(h)$ in the energy norm. The error in the L^2 norm for the DG solution are also given; they are $O(h^2)$ as expected. A discrete L^2 error is computed for the FV region:

$$\|U - u\|_{0,FV} = \left(\sum_{V \in \mathcal{E}_F^h} |V| (U(x_V) - u(x_V))^2 \right)^{1/2}.$$

The rates for the discrete L^2 errors are also $O(h^2)$.

The variable N is the total number of Voronoi cells in the domain Ω . When we increase the degree of approximation in Ω_D to two, the pressure solution is more accurate and the local convergence rate increases to two. This feature is important because it allows for one to use the Discontinuous Galerkin method to obtain accurate solutions on parts of the domain of interest.

Example 2 **Discontinuity in Porous Medium**

In the next example we consider a square domain $\Omega = (0, 2) \times (0, 2)$ with an enclosed triangular domain (see Fig. 3 left). The diffusion coefficient K is equal to 0.01 in the triangular subdomain and 1.0 in the rest of the domain. We impose zero Dirichlet boundary conditions and the source function

$$f(x, y) = -2.0(x^2 - 2x) + (y^2 - 2y).$$

The challenge for the finite volume method in this case arises from the discontinuity

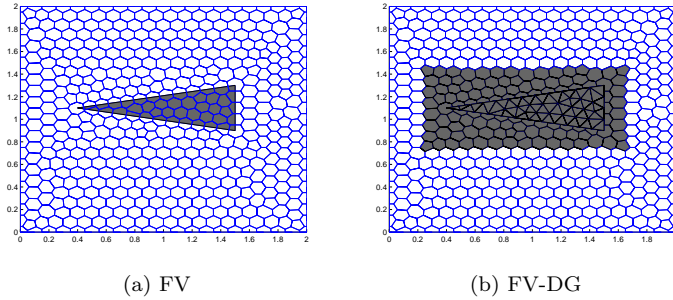


Fig. 3: Computational meshes in the case of triangular inclusion (grey region in left figure). The DG region is a larger rectangular region that contains the triangular inclusion (grey region in right figure).

in the permeability of the porous medium that changes rapidly over a small part of the domain. We want to compare the FV solution with the FV-DG solution on the domains shown in Fig. 3. We first solve the problem on a mesh with 1985 Voronoi cells using the finite volume method on the mesh shown in Fig. 3(a). The solution is shown in Fig. 4 (a) and (c). It is clear the the finite volume solution captures the low permeability in the triangular domain, however it is difficult to obtain an accurate solution as indicated by the three-dimensional plot. Next we solve the problem by using the DG method with parameters $\epsilon = \sigma = 1$ and $r = 2$ in the rectangular shaded region that includes the triangular region as shown in Fig. 3(b). The mesh is a combination of Voronoi cells and triangular elements. The flexibility of DG easily allows the use of hybrid meshes, that can capture the discontinuity interface. The solution is shown in Fig. 4 (b) and (d). We observe that we are able to obtain a more accurate representation of the solution in contrast to the case when the finite volume method is used throughout the domain. This is explained partially by the fact that we have a higher order approximation in the DG region. The FV-DG solution is obtained by solving a problem of size 6509 which as expected is larger than the problem size from the FV solution. We note that solving this problem using the discontinuous Galerkin method on the whole domain yields a problem of size 13734. In this case we have shown that with prior knowledge of the domain, we can choose carefully parts of the domain to use the DG method resulting in an accurate solution in the areas interest. The size of the linear system we solve for the FV-DG coupling in this example and others discussed in this paper is relatively small compared to using the DG method throughout the domain. We believe that this feature works well for applications to porous media flow. Fractures and pinches are

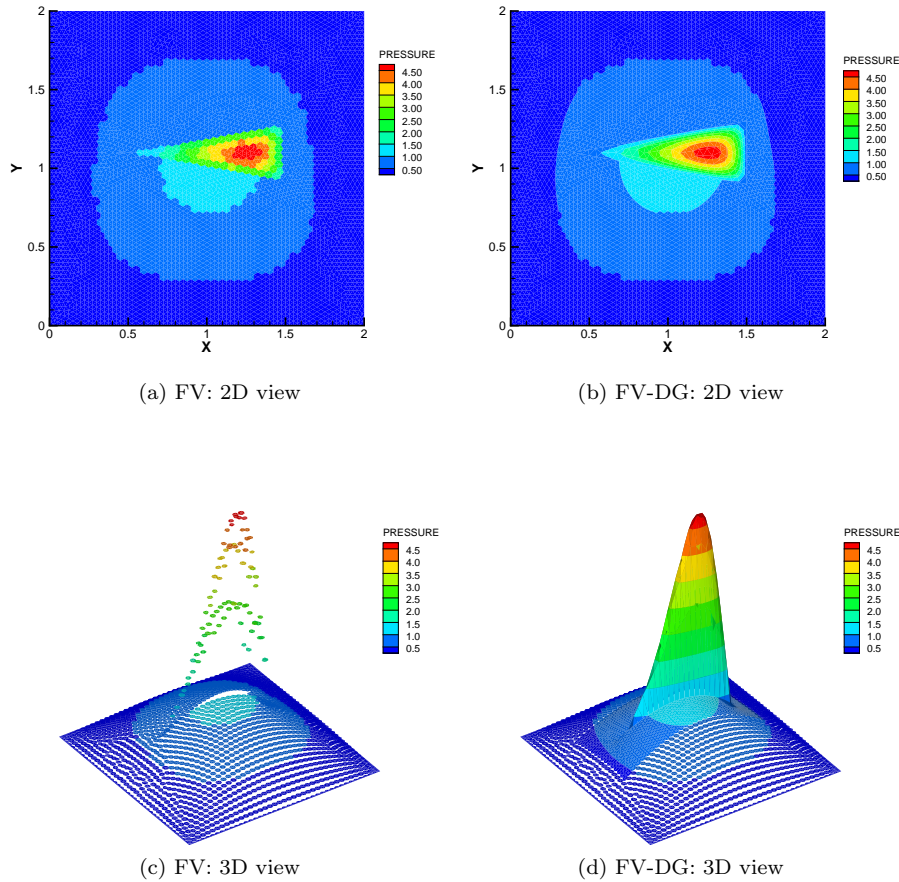


Fig. 4: Contours of pressure solution for example 2

often areas of interest in the flow problem. Since they often occupy small portions of the domain, the proposed coupling can lead to more accurate solutions in these areas at a relatively low computational cost.

Example 3 Anisotropic Diffusion Problem

In the following example we consider a domain $\Omega = (0, 2) \times (0, 2)$ that contains a rectangular subdomain with an anisotropic diffusion matrix (see Fig. 5), instead of a simple diffusion scalar. This example is motivated by a benchmark problem described in [20]. The diffusion matrix is defined by

$$\mathbf{K} = \mathbf{R}_\phi \begin{pmatrix} 1 & 0 \\ 0 & \delta \end{pmatrix} \mathbf{R}_\phi^{-1},$$

where \mathbf{R}_ϕ is the rotation matrix (with $\phi = 30$ degrees) and $\delta = 10^{-3}$ in the shaded triangulated region of the domain (see Fig. 5) and $\delta = 1$ on the rest of the domain.

We solve the problem using the discontinuous Galerkin method in the shaded region in Fig. 5 with parameters $\sigma = \epsilon = 1$ and $r = 2$. We note that other types of finite volume methods can be used to solve problems with anisotropic diffusion coefficients for example [18, 19]. These methods are relatively more complicated to implement because they involve the construction of a discrete gradient. In practice for the finite volume method discussed in this paper one can align the computational grid to the principal directions the flow. This approach is strenuous and easily gets complicated in cases involving changes in the direction of the flow.

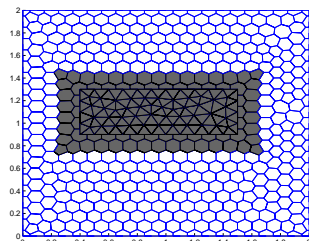


Fig. 5: Computational mesh for example 3: $\delta = 10^{-3}$ in the triangulated grey region and $\delta = 1$ in region partitioned into Voronoi cells.

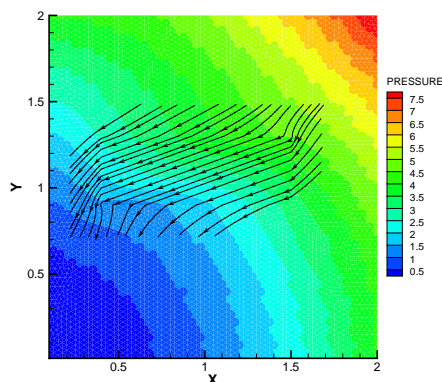


Fig. 6: Contours of pressure solution for example 3. Streamlines are only shown in the DG region.

Fig. 6 shows the pressure contours obtained from the proposed FV-DG scheme. We also plot some of the streamlines located in the DG region only. We can clearly see the oblique flow in the rectangular subdomain due to the anisotropic diffusion tensor.

5 Conclusions

The coupling of discontinuous Galerkin and finite volume methods seems very natural, as both methods share several appealing features. Some may even argue that DG is an extension of FV to high order approximation. This work presents both theoretical and numerical results that confirm the convergence of the multi-numeric algorithm. The resulting solution is more accurate than the finite volume solution, and is less computationally costly than the discontinuous Galerkin solution.

References

1. R.E. Bank and D.J. Bose. Error estimates for the box method. *SIAM J. Numer. Anal.*, 24:777–790, 1986.
2. P. Bastian and B. Riviere. Discontinuous Galerkin methods for two-phase flow in porous media. Technical Report 2004-28, University of Heidelberg, 2004.
3. Z. Cai. On the finite volume element method. *Numer. Math.*, 58:713–735, 1991.
4. Z. Cai, J. Mandel, and S.Mc Cormick. The finite volume element method for diffusion equations on general triangulations. *SIAM J. Numer. Anal.*, 28:392–402, 1991.
5. Y. Epshteyn and B. Riviere. Fully implicit discontinuous finite element methods for two-phase flow. *Applied Numerical Mathematics*, 57:383–401, 2007.
6. R. Eymard, T. Gallouët, and R. Herbin. *Handbook for Numerical Analysis Spaces*. North Holland, 2000.
7. P.A. Forsyth. A control volume finite element approach to NAPL groundwater contamination. *SIAM J. Sci. Statist. Comput.*, 12:1029–1057, 1991.
8. P.A. Forsyth and P.H. Sammon. Quadratic convergence for cell-centered grids. *Appl. Numer. Math.*, 4:377–394, 1988.
9. R. Herbin. An error estimate for a finite volume scheme for a diffusion-convection problem on a triangular mesh. *Numer. Meth. Partial Diff. Equations*, 11:165–173, 1995.
10. R.D. Lazarov, I.D. Mishev, and P.S. Vassilevski. Finite volume methods for convection-diffusion problems. *SIAM J. Numer. Anal.*, 33:31–55, 1996.
11. B. Li, Z. Chen, and G. Huan. Control volume function approximation methods and their applications to modeling porous media flow I: the two-phase flow. *Adv. Water Resources*, 26:435–444, 2003.
12. B. Li, Z. Chen, and G. Huan. Control volume function approximation methods and their applications to modeling porous media flow II: the black oil model. *Adv. Water Resources*, 27:99–120, 2004.
13. A. Michel. A finite volume scheme for the simulation of two-phase incompressible flow in porous media. *SIAM J. Numer. Anal.*, 41:1301–1317, 2003.
14. I.D. Mishev. Finite Volume methods on Voronoi meshes. *Numerical methods for Partial Differential equations*, 14:193–212, 1998.
15. D. Nayagum, G. Schäfer, and R. Mosé. Modelling two-phase incompressible flow in porous media using mixed hybrid and discontinuous finite elements. *Computational Geosciences*, 8:49–73, 2004.
16. B. Niceno. Easymesh. <http://www-dinma.units.it/nirftc/research/easymesh/easymesh.html>.
17. J. Niessner and R. Helmig. Multi-scale modeling of three-phasethree-component processes in heterogeneous porous media. *Advances in Water Resources*, 30:2309–2325, 2007.
18. R.Eymard, T.Gallout, and R. Herbin. A cell-centered finite volume approximation for anisotropic operators on unstructured meshes in any space dimension. *IMA Journal of Numerical Analysis*, 26(2):326–353, 2006.
19. R.Eymard, T.Gallout, and R. Herbin. A new finite volume scheme for anisotropic diffusion problems on general grids: convergence analysis. *Comptes Rendus Mathematique*, 344(6):403 – 406, 2007.
20. R.Herbin and F. Hubert. Benchmark on discretization schemes for anisotropic diffusion problems on general grids. *Finite Volumes for Complex Applications V*, R. Eymard and J-M Herard eds, pages 659–692, 2008.
21. B. Riviere. Numerical study of a discontinuous Galerkin method for incompressible two-phase flow. In *Proceedings of ECCOMAS 2004*, 2004. Available on CD-ROM.

22. B. Riviere. *Discontinuous Galerkin Methods for Solving Elliptic and Parabolic Equations: Theory and Implementation*. SIAM, 2008.
23. B. Riviere, M.F. Wheeler, and K. Banas. Part II. Discontinuous Galerkin method applied to a single phase flow in porous media. *Computational Geosciences*, 4:337–349, 2000.
24. B. Riviere, M.F. Wheeler, and V. Girault. Improved energy estimates for interior penalty, constrained and discontinuous Galerkin methods for elliptic problems. Part I. *Computational Geosciences*, 3:337–360, 1999.
25. P.S. Vassilevski, S.I. Petrova, and R.D. Lazarov. Finite difference schemes on triangular cell-centered grids with local refinement. *SIAM J. Sci. Statist. Comput.*, 13:1287–1313, 1992.